ARTICLE IN PRESS

Bioorganic & Medicinal Chemistry Letters xxx (xxxx) xxxx

Contents lists available at ScienceDirect

Bioorganic & Medicinal Chemistry Letters

journal homepage: www.elsevier.com/locate/bmcl

# SAR studies of 4-acyl-1,6-dialkylpiperazin-2-one arenavirus cell entry inhibitors

Michael B. Plewe[a], Landon R. Whitby[b], Shibani Naik[a], Eric R. Brown[a], Nadezda V. Sokolova[a], Vidyasagar Reddy Gantla[a], Joanne York[d], Jack H. Nunberg[d], Lihong Zhang[e], Birte Kalveram[e], Alexander N. Freiberg[e,f], Dale L. Boger[b,c], Greg Henkel[a], Ken McCormack[a,*]

[a] Arisan Therapeutics, 11189 Sorrento Valley Rd, Suite 104, San Diego, CA 92054, United States
[b] Department of Chemistry, The Scripps Research Institute, 10550 North Torrey Pines Road, La Jolla, CA 92037, United States
[c] The Skaggs Institute for Chemical Biology, The Scripps Research Institute, 10550 North Torrey Pines Road, La Jolla, CA 92037, United States
[d] Montana Biotechnology Center, The University of Montana, Missoula, MT 59812, United States
[e] Department of Pathology, The University of Texas Medical Branch, Galveston, TX 77555, United States
[f] Center for Biodefense and Emerging Infectious Diseases, The University of Texas Medical Branch, Galveston, TX 77555, United States

ARTICLE INFO

*Keywords:*
Arenavirus
Lassa
Junin
Machupo
Piperazinone
Entry inhibitor

ABSTRACT

Old World (Africa) and New World (South America) arenaviruses are associated with human hemorrhagic fevers. Efforts to develop small molecule therapeutics have yielded several chemical series including the 4-acyl-1,6-dialkylpiperazin-2-ones. Herein, we describe an extensive exploration of this chemotype. In initial Phase I studies, $R^1$ and $R^4$ scanning libraries were assayed to identify potent substituents against Old World (Lassa) virus. In subsequent Phase II studies, $R^6$ substituents and iterative $R^1$, $R^4$ and $R^6$ substituent combinations were evaluated to obtain compounds with improved Lassa and New World (Machupo, Junin, and Tacaribe) arenavirus inhibitory activity, *in vitro* human liver microsome metabolic stability and aqueous solubility.

The *Arenaviridae* family of viruses is comprised of a large number of species, some of which are associated with acute hemorrhagic fevers (HF) in humans.[1–3] HF arenaviruses, including Lassa (LASV) and the New World species Machupo (MACV) or Junin (JUNV), represent a serious public health risk, especially in endemic regions of Africa and South America.[4–6] Due to the high mortality rates and limited therapeutic options these HF viruses are classified as Category A pathogens by the Centers for Disease Control (CDC).[7] LASV, in particular, may be responsible for up to 300,000 human disease cases per year.[8–10] Mortality rates for hospitalized LASV HF patients are 15–20% and survivors often suffer permanent sequelae including bilateral hearing damage.[11–14] The nonspecific antiviral Ribavirin currently offers the sole therapeutic option, however, its use is restricted to high-risk patients due to its variable efficacy and potentially serious adverse effects.[15–17] The development of potent and specific agents to treat Lassa and other arenavirus hemorrhagic fevers is therefore, urgently needed.

To mitigate the significant safety and logistical challenges associated with utilizing Biosafety Level 4 (BSL4) arenaviruses in drug discovery, a number of surrogate BSL2 assays have been developed. For example, a screening campaign using the New World arenavirus Tacaribe virus (TCRV), which is a BSL2 Clade B New World arenavirus that is highly-related to Category BSL4 arenaviruses including JUNV and MACV, was used to identify a novel chemical series (including ST-294) of arenavirus inhibitors.[18] Cell-based assays specifically targeting the arenavirus glycoprotein (GP) and cell entry, including pseudotyped virus and cell–cell membrane fusion assays, have also been used to identify or characterize the benzimidazole and 4-acyl-1,6-dialkylpiperazin-2-one chemical series, which share a common GP binding site and mechanism of action.[19–23]

The initial report of the 4-acyl-1,6-dialkylpiperazin-2-one inhibitors identified a set of substituents at the $R^1$, $R^4$ and $R^6$ positions of the 4-acyl-piperazin-2-one core (Fig. 1) that exhibited low micromolar to submicromolar potency against LASV glycoprotein expressed in *vesicular stomatitis virus* (VSV) pseudotyped viruses (pLASV).[20,24,25] Additional investigation of the structure–activity relationships (SAR) of this chemical series identified the carbonyl groups as significant activity determinants and that the enantiomer possessing (*S*) configuration at $C^6$ ($R^6$ group attachment point) was approximately 15-fold more potent than the (*R*)-enantiomer.[26] The (*S*)-enantiomers of our initial 4-acyl-1,6-dialkylpiperazin-2-one compounds **1** (16G8) and **2** (17D1) represent eutomers with pLASV $EC_{50}$ values: *rac*-16G8 600 nM vs (*S*)-16G8 300 nM and *rac*-17D1 500 nM vs (*S*)-17D1 250 nM.[26,27] We

* Corresponding author.
*E-mail address:* kenm@arisanthera.com (K. McCormack).

https://doi.org/10.1016/j.bmcl.2019.08.024
Received 20 April 2019; Received in revised form 10 August 2019; Accepted 11 August 2019
0960-894X/ 

Please cite this article as: Michael B. Plewe, et al., Bioorganic & Medicinal Chemistry Letters, https://doi.org/10.1016/j.bmcl.2019.08.024

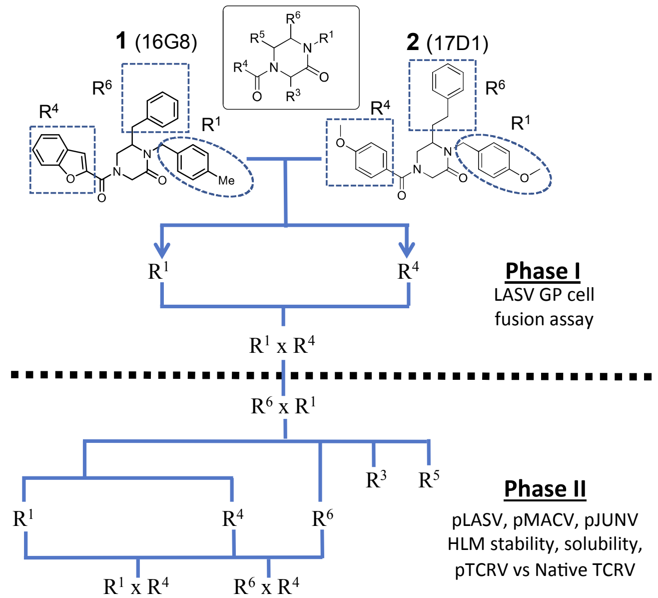


**Fig. 1.** Initial 4-acyl-1,6-dialkylpiperazin-2-one starting points and optimization flow scheme.

therefore utilized the (*S*)-enantiomers of $R^6$ benzyl, phenethyl and other substituents as starting points for further SAR exploration of this chemical series.

In Phase I exploration $R^1$ and $R^4$ scanning libraries were synthesized and screened for inhibition of LASV cell entry as determined in a membrane cell–cell fusion assay at 50 nM (Fig. 1). In Phase II studies, iterative SAR modifications at substituent positions $R^1$, $R^4$ and $R^6$ were evaluated in assays with pseudotyped pLASV, pMACV or pJUNV virions expressing LASV, MACV or JUNV glycoproteins, respectively, in order to identify broad-spectrum arenavirus cell entry inhibitors. Selected compounds were subsequently characterized in human liver microsome (HLM) metabolism and solubility assays (Fig. 1).

For $R^1$ scanning library compounds we devised a synthetic route enabling final step diversification at the $R^1$ position starting with an intermolecular Mitsunobu alkylation[28] of *t*-butyl nosylglycine with Boc protected aminoalcohol **A** to provide **B** (Scheme 1). The nosyl group was cleaved (thiophenol, $K_2CO_3$, DMF) to yield the secondary amine **C**, which was then coupled with the appropriate carboxylic acid $R^4$COOH (EDCI, HOAt, 2,6-lutidine, DMF) to give the tertiary amide **D**. Hydrolysis of the *t*-butyl ester (LiOH, *t*-BuOH/$H_2O$/THF) followed by Boc-deprotection with TFA ($CH_2Cl_2$) provided the amino acid **E** as the TFA salt. Final step diversification at $R^1$ was completed through a one-pot reductive amination[29]/EDCI-mediated ring closure starting with intermediate **E**.

A synthetic route enabling final step diversification at the $R^4$

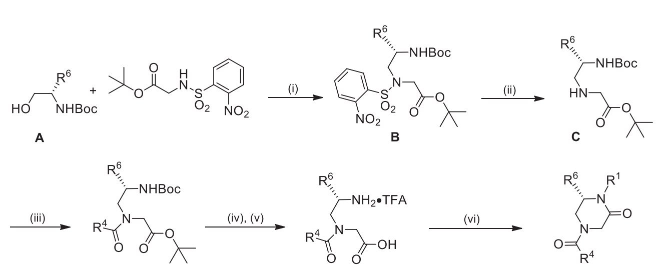

**Scheme 1.** Reagents and conditions: (i) $PPh_3$, DIAD, THF, under $N_2$, rt, 2 h; (ii) PhSH, $K_2CO_3$, DMF, under $N_2$, rt, 3 h; (iii) $R^4$COOH, HOAt, 2,6-lutidine, EDCI, DMF, rt, 16 h; (iv) LiOH, *t*-BuOH/$H_2O$/THF, rt, 1 h, then 1 N aq. HCl; (v) TFA, $CH_2Cl_2$, rt; (vi) RCHO, $NaBH(OAc)_3$, $Et_3N$, $ClCH_2CH_2Cl$, rt, 18 h, then EDCI, $NaHCO_3$, $CH_2Cl_2$, rt, 8 h.

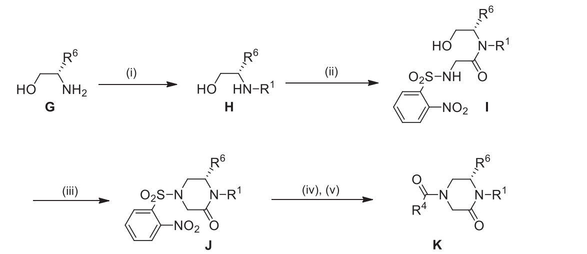

**Scheme 2.** Reagents and conditions: (i) RCHO, MeOH, rt, 1 h, then $NaBH_4$, 0 °C to rt, 2 h; (ii) 2-(2-nitrophenylsulfonamido)acetyl chloride, $NaHCO_3$, $CH_2Cl_2$, rt, 3 h; (iii) $PPh_3$, DIAD, THF, under $N_2$, rt, 2 h; (iv) PhSH, $K_2CO_3$, DMF, under $N_2$, rt, 3 h; (v) $R^4$COOH, HOAt, 2,6-lutidine, EDCI, DMF, rt, 14 h.

position (Scheme 2) started with commercially available aminoalcohol **G**. The $R^1$ group was added using a stepwise reductive amination procedure with appropriate aldehyde entailing pre-formation of imine followed by $NaBH_4$ reduction (MeOH) to give intermediate **H**. Subsequent *N*-acylation by treatment of **H** with the acid chloride of nosylglycine ($NaHCO_3$, $CH_2Cl_2$) provided **I**. The 6-membered ring was closed using an intramolecular Mitsunobu alkylation of the sulfonamide[28] ($PPh_3$, DIAD, THF) to give **J**. Nosyl deprotection using thiophenol and $K_2CO_3$ (DMF) and subsequent acylation of the free amine with the appropriate carboxylic acid $R^4$COOH (EDCI, HOAt, 2,6-lutidine, DMF) furnished compounds of type **K**. All compounds were purified by PTLC or flash chromatography and the purity and identity of all compounds was assessed by LC/MS.

At $R^1$ benzyl was favored over phenethyl or phenylpropyl substituents (Table 1, compare **6**, **14** and **16**), indicating a defined preference for the linker length at $R^1$. A single aryl ring demonstrated greater activity than naphthalene and biaryl groups (compare **6** with **10**, **12**, **13** and **15**) and the identity of aryl substituents significantly impacted activity while their positional effects were relatively weaker. The incorporation of single methoxy or hydroxy groups revealed a preference for *meta*-substitution but were well tolerated at any ring position (**4** vs. **8** and **9**, **5** vs. **7**). In contrast, halogen, phenoxy, cyano, nitro, or basic nitrogen substitutions in the ring significantly reduced activity at any position (see Supplementary data, Fig. S1). Overall, the results indicated significant flexibility for incorporation of small lipophilic substituents or polar alcohols on the $R^1$ benzyl ring.

As opposed to $R^1$ substituents, the $R^4$ acyl substituents demonstrated SAR with strong preferences in both the identity and position of aryl functionality (Table 1, Supplementary data, Fig. S2). The two most active classes of aryl groups observed in the original piperazinone study (the 2-heteroaryl (**17**–**19**, **22**) and the 4-substituted phenyl (**20**, **21**, **23**) groups) proved optimal in the $R^4$ scanning library.[20] Of note, incorporation of an alkoxy or dimethylamino group at the 4-position of the phenyl ring resulted in a notable increase in potency for compounds **20**, **21**, and **23** while the absence of a 4-position substituent (**28**) and/or the placement of a dimethylamino (**29**) or alkoxy (**30**) group at the 3-position resulted in dramatic losses in activity. The addition of a 5-methoxy group to the 2-indole substituent (compounds **17** vs. **26**) also provided a notable increase in potency. In contrast, the addition of a single carbon linker (**27**) to the phenyl ring significantly decreased activity.

Following the individual $R^1$ and $R^4$ replacements, a small combinatorial library was synthesized containing three of the most active $R^1$ substituents (compounds **3**–**5**, Table 1) and $R^4$ acyl groups (compounds **17**, **18**, and **20**, Table 1). These compounds showed low-nanomolar inhibition of LASV GP fusion with no loss of activity when the more polar optimal substituents were combined in the same structure (compounds **31**–**33**, Table 2) suggesting that optimization for lipophilic efficiency (LipE) may lead to potent compounds with improved drug-like properties. These initial scanning libraries allowed the identification of promising $R^1$ and $R^4$ substituents as starting points to initiate optimization of broad-spectrum arenavirus inhibitory activity and drug-like

**Table 1**
SAR data of selected $R^1$ (left panel) and $R^4$ (right panel) substituent Phase I scanning libraries indicating their % inhibition at 50 nM in the LASV GPC cell–cell fusion assay.

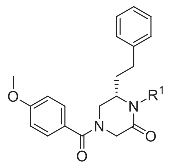
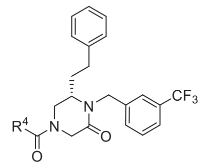

| Compd. | $R^1$ | % inh. 50 nM | Compd. | $R^4$ | % inh. 50 nM |
|---|---|---|---|---|---|
| **3** | 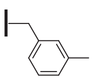 | 86 | **17** | 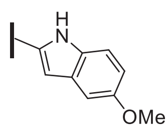 | 66 |
| **4** | 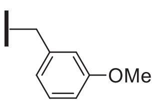 | 82 | **18** | 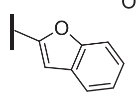 | 61 |
| **5** | 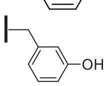 | 81 | **19** | 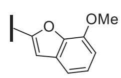 | 59 |
| **6** | 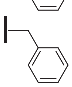 | 71 | **20** | 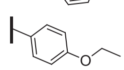 | 58 |
| **7** | 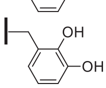 | 64 | **21** | 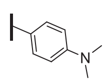 | 56 |
| **8** | 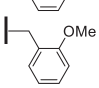 | 61 | **22** | 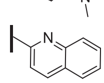 | 54 |
| **9** | 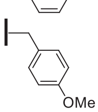 | 60 | **23** | 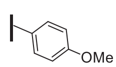 | 50 |
| **10** | 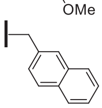 | 58 | **24** | 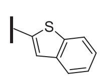 | 45 |
| **11** | 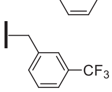 | 53 | **25** | 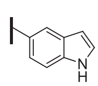 | 40 |
| **12** | 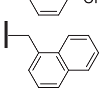 | 51 | **26** | 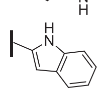 | 26 |
| **13** | 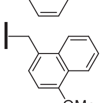 | 36 | **27** | 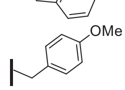 | 18 |
| **14** | 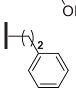 | 34 | **28** | 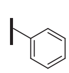 | 15 |
| **15** | 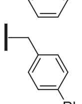 | 33 | **29** | 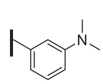 | 14 |
| **16** | 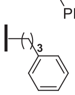 | 31 | **30** | 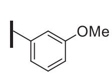 | 0 |

properties.

Phase II SAR exploration studies, including characterization of broad-spectrum arenavirus (pseudotyped pLASV, pMACV and pJUNV) activity, human liver microsome (HLM) metabolic stability and solubility, were initiated with the synthesis of analogs containing benzyl or phenethyl at $R^6$, benzyl or *m*-methoxy benzyl at $R^1$ and 5-methoxyindole at $R^4$. $R^6$ phenethyl was found to exhibit approximately 2–4 fold greater potency over benzyl (Table 3, compare **35**, **40**, **41** and **42**). However, $R^6$ benzyl compounds exhibited greater solubility and metabolic stability in HLM assays. Thus, while **42** was 2–4 fold less potent in pLASV, pMACV and pJUNV assays than **41** it exhibited a substantially increased HLM half-life of 59 vs 10 min and solubility of 36 vs 4 µM.

For Phase II SAR expansion we synthesized $R^6$ (*S*) benzyl analogs with a limited number of $R^4$ substituents (5-methoxy, 5-methyl, and 5-cyclopropyl indoles) to further explore $R^1$ SAR (80 analogs) as well as a limited number of $R^1$ substituents (benzyl, *m*-methoxybenzyl, *m*-isopropoxybenzyl, or *m*-difluoromethoxybenzyl) to explore additional $R^4$ SAR (68 analogs), respectively. Novel $R^6$ SAR was also explored utilizing a limited number of $R^1$ and $R^4$ substituents (64 analogs). In total 212 additional analogs were synthesized in Phase II modifications at $R^1$, $R^4$ and $R^6$.

All Phase II analogs were first screened against pLASV and pMACV. Those exhibiting $EC_{50}$ values < 25 nM in both assays were subsequently tested against pJUNV. Of the 132 of compounds displaying < 25 nM potency in the pLASV assay, 118 were also < 25 nM against pMACV and of those 108 were also < 25 nM against pJUNV. Comparative $EC_{50}$ values and the range of activity spectrums for these Phase II analogs are illustrated in Fig. 2. While a number of interesting pseudotyped-specific SAR trends were observed, our focus was on the identification of compounds exhibiting broad spectrum activity with $EC_{50}$ values < 10 nM in all three assays (64 compounds).

To confirm that the activities observed in pseudotyped virus assays translate to the inhibition of replicative arenaviruses the activities of two compounds (**35** and **42**, Table 3) were initially tested and confirmed against BSL4 replicative LASV with $EC_{50}$ values of 33 and 113 nM, respectively. To extend this observation to a broader range of compounds we subsequently tested compounds exhibiting $EC_{50}$ values < 25 nM against pLASV, pMACV and pJUNV in assays with both pseudotyped (p-TCRV) and replicative Tacaribe (TCRV) virus, a BLS2 virus that is non-pathogenic to humans but highly related to JUNV.[18] As shown in Fig. 3 compounds exhibiting < 25 nM $EC_{50}$ values against the BSL4 pseudotyped viruses also exhibited comparable activities against pTCRV. These data confirm comparable inhibition between the glycoprotein-mediated cell entry of both the BSL4 and BSL2 viruses. Furthermore, the data confirm the translation between pseudotyped and replicative virus inhibition ($R^2 = 0.61$, Fig. 3). Thus, the data further validate the selection of cell entry inhibitors based on their activities in pseudotyped virus assays.

At $R^1$, SAR trends were observed in both antiviral activity and HLM stability (Table 4). Benzyl groups with less polar meta- or ortho- substituents are consistently potent and broad spectrum (compounds **40**, **43**, **44**, **45**, **48**, and **49**) with a particular preference for lipophilic ethers. Some polar $R^1$ *meta*-benzyl substituents groups including alcohols (compounds **52**, **56**, and **59**), retain broad spectrum activity despite their increased polarity while others such as sulfonamides (**54**), and moderately polar groups like 1H-pyrazolyl (**53**) and alkyl esters (**55**) retain pMACV and pJUNV activity but lose activity against pLASV. Both carboxylic acids and amides (compounds **60** and **61**) are not tolerated for any viral species tested (see data for more analogs in Supplementary data, Table S1).

Unfortunately, alkyl ethers at $R^1$ pose a significant metabolic liability as demonstrated by the relative HLM stability of compounds **42** and **43** vs. **40**, **44** and **45**. Stabilized ethers with oxidation-resistant alkyl groups (compounds **46** and **47**) have more favorable microsome stability but only the *m*-difluoromethoxy (**46**) group maintains broad-spectrum activity. The broad-spectrum nature of *m*-difluoromethoxy group is interesting in light of the poor pJUNV and pMACV activity of more lipophilic *m*-trifluoromethoxy (**47**) analog and the general preference for alcohols as $R^1$ substituents, as the difluoromethoxy group has been reported to act as a hydrogen-bond donor and potential isostere for alcohols.[30]

**Table 2**
Analogs incorporating combinations of the most active substituents from the R[1] and R[4] scanning libraries and their respective $EC_{50}$ values in the LASV GPC cell–cell fusion assay.

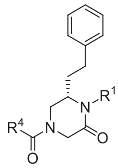

| $R^4$ | $R^1$ | | | | | |
|---|---|---|---|---|---|---|
| | 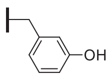 | | 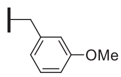 | | 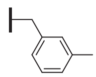 | |
| | Compd. | $EC_{50}$ (nM) | Compd. | $EC_{50}$ (nM) | Compd. | $EC_{50}$ (nM) |
| 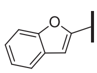 | **31** | 5 | **34** | 4 | **37** | 5 |
| 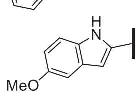 | **32** | 8 | **35** | 7 | **38** | 7 |
| 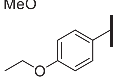 | **33** | 7 | **36** | 6 | **39** | 5 |

Both 6-indolyl (**50**) and *N*-alkyl 6-indolyl groups (**51, 57, 58**) also demonstrate good broad-spectrum activity, but the highest activity is derived from the unalkylated analog **50**. This is likely due to the hydrogen bonding of indole N—H, similar to the phenols and $-OCF_2H$ groups. The unalkylated indoles also possess above average metabolic stability with **50** having an HLM half-life ($T_{1/2}$) of 36 min, while introduction of alkyl groups causes significant metabolic liability.

Novel $R^4$ analogs were synthesized using the metabolically more stable $R^1$ groups benzyl and *m*-difluoromethoxy benzyl to further evaluate potential metabolic liabilities stemming from the $R^4$ substituent (Table 5). The majority of Phase II $R^4$ analogs were designed to explore substituents on the most potent aryl and heteroaryl $R^4$ groups (indoles, phenyls, and quinolines) identified in the Phase I exploration, with the intention of further improving metabolic stability while retaining broad-spectrum potency. Although some sterically bulky 5-alkoxy indoles showed dramatic improvements in metabolic stability (compounds **62** and **63**) broad-spectrum potency was lost. 5-methylindole and 5-cyclopropylindole substituents (compounds **68** and **69**) demonstrated sufficiently increased metabolic stability over 5-methoxyindole analog (**42**), when paired with a benzyl $R^1$. Of note, compound **66** having 5-cyclopropylindole at $R^4$ and *m*-difluoromethoxy benzyl at $R^1$ showed some improvement in metabolic stability but at the same time was slightly less potent than the 5-methoxyindole analog **46** (see Table 4).

The 7-fold difference in potency against pLASV between **66** and **69** strongly suggested that it should be possible to pair 5-cyclopropylindole and a suitable $R^1$ group to obtain a broadly potent compound that maintained the cyclopropylindole's metabolic stability gains. While other heteroaryl groups showed acceptable-to-good broad-spectrum potency, such as quinolines **67** and **73** and benzothiophene **71**, none of them were found to endow stability or solubility advantages over the indole. Further, the wide range of 4-substituted phenyls synthesized showed significantly reduced broad-spectrum activity with few exceptions, e.g., the 4-piperidinylphenyl group (**75**), which while potent, exhibited an HLM half-life of only 5 min. Polar substituents such as sulfones (**72**, **74**), nitriles (**70**), acetyl (**65**, **76**) and a variety of other groups were not tolerated on either phenyl or heteroaryl rings at any position and lead to dramatically reduced potency (see Supplementary data, Table S2). 5-methyl and 5-cyclopropyl indoles were thus selected as the preferred $R^4$ groups to generate $R^1$ and $R^6$ combinatorial compounds optimized for stability and potency.

In parallel with expansion of $R^1$ and $R^4$ SAR we explored additional

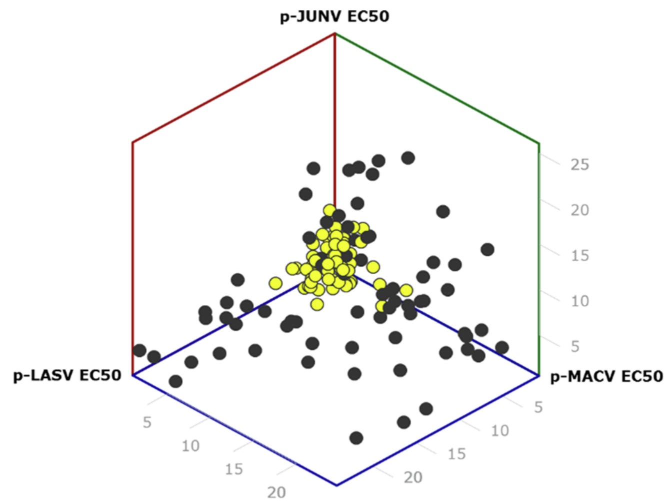


**Fig. 2.** A 3-dimensional plot of $EC_{50}$ values obtained in the pLASV, pMACV and pJUNV assays for the analogs exhibiting < 25 nM (dark circles) or < 10 nM (yellow circles) $EC_{50}$ values in each of the pseudtoyped virus assays.

**Table 3**
Comparison of activity of $R^6$ linker length and $R^1$ substituents. Activity is given as $EC_{50}$ (nM) in the indicated pseudotyped virus assays. Cytotoxicity is given as $CC_{50}$ in Vero cells (7 days). HLM data is the observed half-life ($T_{1/2}$ (min)) in a human liver microsome assay. Aqueous solubility (μM) was measured at pH 7.4.

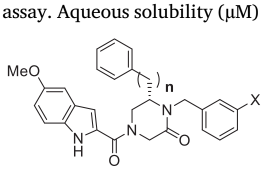

| Compd. | n | X | p-LASV | p-MACV | p-JUNV | $CC_{50}$ (nM) | HLM | Solubility |
|---|---|---|---|---|---|---|---|---|
| **35** | 2 | OMe | 1.74 | 2.39 | 1.77 | 4,500 | 7.7 | 4.9 |
| **40** | 1 | OMe | 6.9 | 3.6 | 2.52 | 3,300 | 9.8 | 7.4 |
| **41** | 2 | H | 3.3 | 2.13 | 5.8 | > 30,000 | 10 | 4.4 |
| **42** | 1 | H | 8.64 | 11.52 | 4.87 | > 10,000 | 59 | 36.3 |

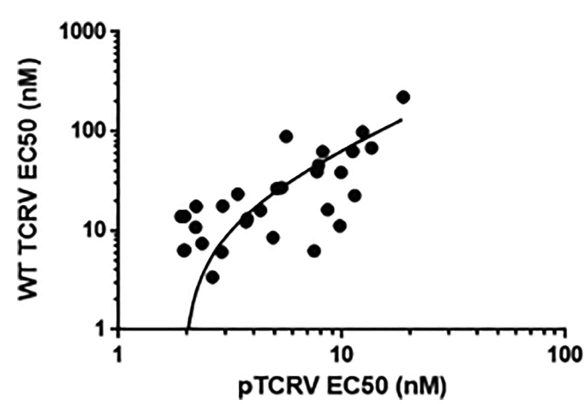


**Fig. 3.** Logarithmic plot of pTCRV vs replicative TCRV (immunostaining assay) $EC_{50}$ values ($R^2$ = 0.61) for analogs selected for $EC_{50}$ values < 25 nM against each of the pseudotyped viruses (pLASV pMACV and pJUNV) and HLM half-life data.

**Table 4**
Phase II SAR of $R^1$ substituents. Activities provided are $EC_{50}$ values (nM) in the indicated pseudotyped virus assays. Cytotoxicity is given as $CC_{50}$ in Vero cells (7 days). HLM data is the observed half-life (minutes) in a human liver microsome assay. Aqueous solubility (μM) was measured at pH 7.4.

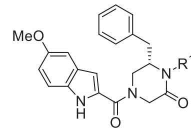


| Compd. | $R^1$ | p-LASV | p-MACV | p-JUNV | $CC_{50}$ (nM) | HLM | Solubility |
|---|---|---|---|---|---|---|---|
| **40** | 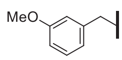 | 6.9 | 3.6 | 2.52 | 3,300 | 9.8 | 7.4 |
| **42** | 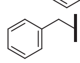 | 8.64 | 11.52 | 4.87 | > 10,000 | 59 | 36.3 |
| **43** | 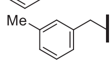 | 2.92 | 2.08 | 3.04 | > 10,000 | 37 | 5.8 |
| **44** | 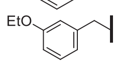 | 1.33 | 1.54 | 1.91 | 41,000 | 12 | 6.9 |
| **45** | 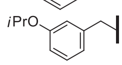 | 2.37 | 2.88 | 3.78 | 49,000 | 8 | 5.7 |
| **46** | 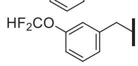 | 0.94 | 1.85 | 0.75 | > 30,000 | 59 | 7.2 |
| **47** | 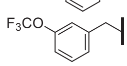 | 5.8 | > 25 | 12.23 | > 30,000 | 72 | 5.6 |
| **48** | 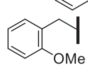 | 5.45 | 2.85 | 1.56 | > 30,000 | 25 | 11.3 |
| **49** | 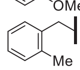 | 5.56 | 6.26 | 11.16 | > 100,000 | 27 | 24.2 |
| **50** | 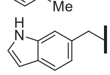 | 0.733 | 1.73 | 2.68 | 5,000 | 36 | 10.21 |
| **51** | 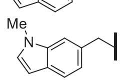 | 4.44 | 1.32 | 3.14 | > 30,000 | 13 | 9.2 |
| **52** | 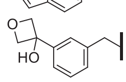 | 2.81 | 3.17 | 6.91 | 79,500 | 11 | 48.8 |
| **53** | 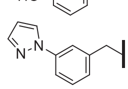 | 22.1 | 1.38 | 1.65 | > 30,000 | N/A | 6.8 |
| **54** | 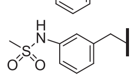 | > 25 | 5.71 | 3.27 | N/A | N/A | 12 |
| **55** | 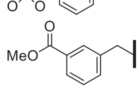 | 23.6 | 5.4 | 1.8 | > 30,000 | N/A | 6.9 |
| **56** | 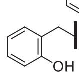 | 2.42 | 2.50 | 5.38 | 10,200 | 18 | 17.2 |
| **57** | 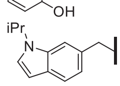 | 3.7 | 2.88 | N/A | > 30,000 | 5.3 | 3.9 |
| **58** | 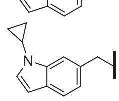 | 2.7 | 2.03 | 2.6 | > 100,000 | 13 | 7.5 |
| **59** | 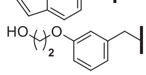 | 4.09 | 1.01 | 1.85 | 39,000 | 29 | 30.2 |
| **60** | 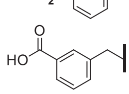 | > 25 | > 25 | N/A | N/A | N/A | N/A |
| **61** | 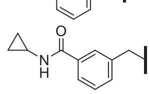 | > 25 | > 25 | N/A | N/A | N/A | N/A |

$R^6$ substituents whereby $R^4$ (5-methoxy indole) and $R^1$ (benzyl, *m*-methoxybenzyl and *m*-difluoromethoxybenzyl) substituents were restricted and novel $R^6$ substituent analogs synthesized. The $R^6$ position is the most tolerant of different substitutions and a wide variety of either lipophilic or polar charged groups were synthesized using either Scheme 1, starting with the appropriate commercially available chiral aminoalcohol, or Scheme 3 with the intention of increasing solubility and metabolic stability concurrently. Thus, methyl (O-*t*-Bu)serinate (**L**) was first acylated with $R^1$COOH and EDCI (Scheme 3). Subsequent reduction of **M** using lithium aluminum hydride afforded aminoalcohol **N**. Acylation of the amine with nosylglycine acyl chloride and magnesium oxide gave intermediate **O**, which was cyclized under Mitsunobu

**Table 5**
Phase II SAR of $R^4$ substituents. Activities provided are $EC_{50}$ values (nM) in the indicated pseudotyped virus assays. Cytotoxicity is given as $CC_{50}$ in Vero cells (7 days). HLM data is the observed half-life ($T_{1/2}$ (min)) in a human liver microsome assay. Aqueous solubility (μM) was measured at pH 7.4.

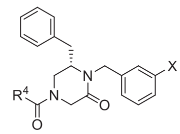


| Compd. | $R^4$ | X | p-LASV | p-MACV | p-JUNV | $CC_{50}$ (nM) | HLM | Solubility |
|---|---|---|---|---|---|---|---|---|
| **42** | 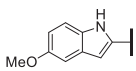 | H | 8.64 | 11.52 | 4.87 | > 10,000 | 59 | 36.3 |
| **62** | 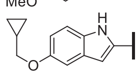 | H | 9.38 | > 25 | > 25 | > 30,000 | 137 | 8.6 |
| **63** | 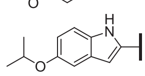 | H | > 25 | > 25 | 4.235 | N/A | 246 | 14.6 |
| **64** | 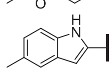 | $OCF_2H$ | 2.34 | 19.52 | 3.8 | > 100,000 | 43 | 5.3 |
| **65** | 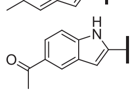 | H | 25.4 | > 25 | > 25 | > 10,000 | 120 | 15.5 |
| **66** | 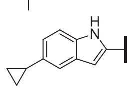 | $OCF_2H$ | 2.12 | 6.81 | 4.05 | 10,400 | 77 | 6.2 |
| **67** | 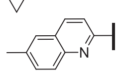 | $OCF_2H$ | 2.29 | 2.99 | 0.52 | 29,700 | 13 | 10 |
| **68** | 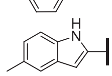 | H | 1.95 | 21.52 | 2.68 | 11,200 | 119 | 7.7 |
| **69** | 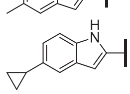 | H | 14.6 | > 25 | > 25 | > 100,000 | 125 | 8.3 |
| **70** | 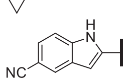 | H | > 25 | > 25 | > 25 | 16,000 | N/A | 10.8 |
| **71** | 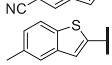 | H | 5.96 | 12.53 | 4.46 | 9,040 | 42 | 5.7 |
| **72** | 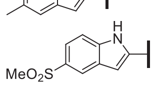 | H | > 25 | > 25 | > 25 | N/A | N/A | 67.7 |
| **73** | 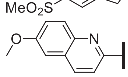 | $OCF_2H$ | 2.31 | 3.59 | 4.78 | > 100,000 | 16 | 9.5 |
| **74** | 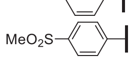 | OMe | > 25 | > 25 | > 25 | N/A | N/A | > 100 |
| **75** | 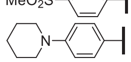 | $OCF_2H$ | 4.68 | 3.98 | 8.82 | 46,700 | 5 | 8.8 |
| **76** | 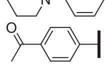 | H | > 25 | > 25 | > 25 | > 100,000 | 31 | > 100 |

conditions to afford piperazinone **P**. Treatment of the *t*-butyl ether with 4 N HCl in 1,4-dioxane gave free alcohol **Q**, which was first triflated using triflic anhydride and finally reacted with a desired amine NHR'R" to afford intermediate **R.** Finally, nosyl deprotection followed by the amide coupling with the appropriate carboxylic acid $R^4COOH$ furnished compounds of type **S**.

For non-polar $R^6$ substituents (Table 6) potency tracks well with lipophilicity and the physical length of the group is unimportant (compounds **77**, **81**, **82**, **83**, and **84**). For $R^6$ analogs bearing a basic amine, a linker length of one carbon between the piperazinone and amine (e.g., **79** vs **94**) is preferred for activity. Overall lipophilicity of the $R^6$ amine is important for activity, as tertiary amines (**90**) with fewer carbons than piperidine, and thus lower lipophilicity, resulted in complete loss of potency. Larger amine groups themselves bearing polar substituents such as sulfones and sulfonamides (**88**, **91**), nitriles (**92**), and even methoxy (**87**) groups all show significant losses in activity. Additionally, the basicity of the amine plays an important role in determining activity, as difluorinated piperidine analogs, which are more lipophilic yet less basic, exhibit decreased activity compared to the unfluorinated parent piperidine (compound **78** vs. **86** and **93**). If the site of fluorination is sufficiently removed from the basic nitrogen, as in the 4-methylpiperidine (**85**) and its 4-trifluoromethyl analog (**89**), the inductive withdrawal effect on basicity is minimized and the increased lipophilicity makes **89** more potent.

The HLM half-life of all compounds in this $R^6$ exploration series was < 50 min, except **79**, which exhibited a half-life of 52 min. Pairing the cyclopropylpiperidine of **79** with an $R^4$ group that is less metabolically labile than 5-methoxy indole could provide further improvement in HLM stability. A number of additional $R^6$ analogs did not exhibit broad-spectrum potency and/or improved HLM stability (see Supplementary data, Table S3).

Initial exploration at positions $R^3$ and $R^5$, as well as attempts to

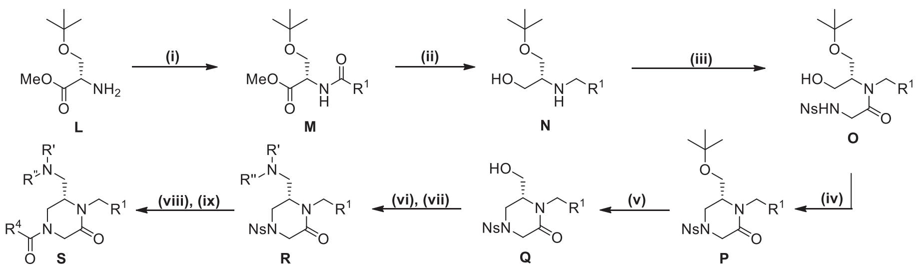

**Scheme 3.** Reagents and conditions: (i) $R^1COOH$, EDCI, $Et_3N$, DCM, rt, 16 h; (ii) LAH, THF, reflux, 16 h; (iii) 2-(2-nitrophenylsulfonamido)acetyl chloride, MgO, 4:1 THF/$H_2O$, rt, 4 h; (iv) $PPh_3$, DIAD, THF, under $N_2$, rt, 16 h; (v) 4 N HCl/1,4-dioxane, 70 °C, 4 h; (vi) $Tf_2O$, $Et_3N$, DCM, under $N_2$, 0 °C, 1 h, then rt, 3 h; (vii) NHR'R", $Et_3N$, THF, rt, 16 h; (viii) PhSH, $K_2CO_3$, DMF, under $N_2$, rt, 16 h; (ix) $R^4COOH$, 2,6-lutidine, EDCI, DMF, rt, 4 h.

**Table 6**

Phase II SAR of $R^6$ substituents. $R^6$ groups bearing amines were synthesized according to Scheme 3. Activities provided are $EC_{50}$ values (nM) in the indicated pseudotyped virus assays. Cytotoxicity is given as $CC_{50}$ in Vero cells (7 days). HLM data is the observed half-life ($T_{1/2}$ (min)) in a human liver microsome assay. Aqueous solubility (μM) was measured at pH 7.4.

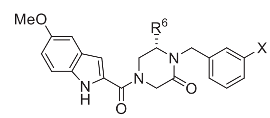

| Compd. | $R^6$ | X | p-LASV | p-MACV | p-JUNV | $CC_{50}$ (nM) | HLM | Solubility |
|---|---|---|---|---|---|---|---|---|
| **77** | 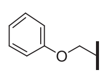 | H | 5.53 | 20.75 | 5.66 | > 10,000 | 39 | 12.2 |
| **78** | 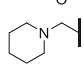 | H | 4.76 | 4.75 | 5.35 | 76,900 | 17 | > 100 |
| **79** | 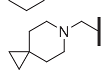 | H | 2.99 | 4.53 | 1.25 | 17,100 | 52 | 28.2 |
| **80** | 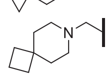 | H | 12.56 | 11.24 | 12.6 | 4,900 | N/A | 11.8 |
| **81** | 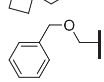 | OMe | 2.7 | 3.38 | 4.65 | > 10,000 | N/A | 11.7 |
| **82** | 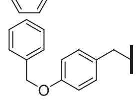 | OMe | 1.34 | 2.66 | 1.14 | > 10,000 | N/A | 3.8 |
| **83** | 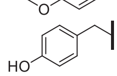 | OMe | 5.56 | 5.08 | 8.05 | > 10,000 | N/A | 11.8 |
| **84** | 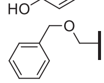 | H | 5.53 | 4.285 | 4.3 | > 30,000 | N/A | 8.8 |
| **85** | 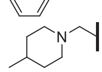 | H | 11.2 | > 25 | 3.15 | > 30,000 | 16 | 93.1 |
| **86** | 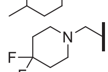 | H | 11.34 | 20.5 | 23.6 | 95,300 | 23 | 72.4 |
| **87** | 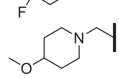 | H | > 25 | > 25 | N/A | N/A | N/A | > 100 |
| **88** | 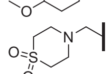 | H | > 25 | > 25 | N/A | N/A | N/A | > 100 |
| **89** | 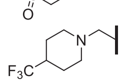 | H | 3.47 | 8.925 | 3.92 | 17,300 | 32.5 | 16.5 |
| **90** | 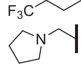 | H | > 25 | > 25 | N/A | N/A | N/A | > 100 |
| **91** | 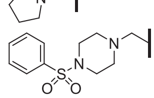 | H | 21.1 | > 25 | 16.2 | N/A | N/A | 16.9 |
| **92** | 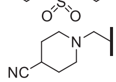 | $OCF_2H$ | 20.69 | 23.24 | > 25 | N/A | N/A | 27.9 |
| **93** | 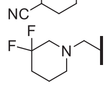 | $OCF_2H$ | 20.25 | 25.52 | 32.7 | > 100,000 | N/A | 53.1 |
| **94** | 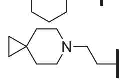 | H | > 25 | > 25 | > 25 | N/A | N/A | > 100 |

conformationally lock the position of the $R^4$ or $R^1$ substituents (see Supplementary data, Table S4 and Fig. S3) were unable to identify suitably active chemical subseries. Thus, final analog series were synthesized to identify additional $R^1$ (Table 7, Supplementary data, Table S5) and $R^6$ (Table 8) modifications in combination with the most stable, broadly potent complementary $R^4$, $R^6$ and $R^1$ groups. Combining preferred $R^1$ substituents with the 5-methylindole and 5-cyclopropylindole moieties gave a series of compounds with attractive broad-spectrum potency and improved stability.

The most active polar compounds in this set (Table 7, compounds **99**, **100**, **103**, and **104**) contain $R^1$ groups with benzyl alcohol substituents, as previously suggested by the Phase I and II $R^1$ explorations. While the benzyl alcohols proved to be metabolically labile *m*-alkyl substituted groups (**96**, **101**) provided moderate HLM stability. Compound **102,** containing the 6-indolyl group, demonstrated broad-spectrum potency and an excellent HLM half-life of 187 min. Unfortunately, additional combinations of selected metabolically stable $R^1$ (benzyl) and $R^4$ groups (5-methylindole and 5-cyclopropylindole) with $R^6$ amines intended to increase aqueous solubility did not prove advantageous for either solubility or broad-spectrum antiviral activity (Table 8, compounds **105–108**).

In a final functional assay the prioritized compounds (Table 9) were also tested against pseudotyped virus expressing the GP of an attenuated JUNV strain (Candid-1). Each of these analogs exhibited decreased potencies against pJUNV (Candid-1) vs pJUNV, ranging from > 10- (**98**) to nearly 1000-fold (**46**). Interestingly, the attenuating mutation (F427I) in the GP of Junin (Candid-1) virus also exhibits resistance to benzimidazole cell entry inhibitors.[31,32] Consistent with earlier reports that the 4-acyl-1,6-dialkylpiperazin-2-one and benzimidazole chemical series share a common GP binding site and mechanism of action our results indicate that these distinct chemical series also share at least some resistance variants associated with attenuation.[22,23,31]

In summary, the SAR exploration and optimization of 4-acyl-1,6-dialkylpiperazin-2-one chemical series was initiated with the (*S*)-enantiomers of compounds **1** and **2** exhibiting pLASV $EC_{50}$ values in the 250–300 nM range.[26] In the current study we generated analogs with up to ~100-fold greater potency including low to sub-nanomolar broad spectrum activity against Old (pLASV) and New World (pMACV, pJUNV and pTCRV) pseudotyped viruses that translate to activity against replicative Lassa and Tacaribe viruses. Attempts to substantially increase solubility while maintaining broad-spectrum potency and other drug like properties met with limited success. However, novel $R^1$, $R^4$ and $R^6$ substituent combinations that improved the HLM metabolic half-lives from < 10 min in our initial broad-spectrum compounds to > 45 min were identified for a subset of analogs. Those compounds exhibiting broad-spectrum arenavirus activity with $EC_{50}$ values ≤10 nM against each of the pseudotyped viruses and HLM half-lives of > 45 min (Table 9) may be prioritized for further evaluation and advancement.

**Table 7**
Secondary Phase II synthesis and SAR of $R^1$ analogs combined with selected $R^4$ and benzyl $R^6$ groups. Activities provided are $EC_{50}$ values (nM) in the indicated pseudotyped virus assays. Cytotoxicity is given as $CC_{50}$ in Vero cells (7 days). HLM data is the observed half-life ($T_{1/2}$ (min)) in a human liver microsome assay. Aqueous solubility (μM) was measured at pH 7.4.

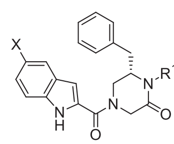


| Compd. | $R^1$ | X | p-LASV | p-MACV | p-JUNV | $CC_{50}$ (nM) | HLM | Solubility |
|---|---|---|---|---|---|---|---|---|
| **95** | 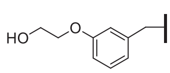 | 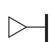 | 7.72 | 1.08 | 2.16 | 4,300 | 50 | 9.4 |
| **96** | 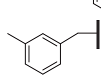 | 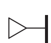 | 0.94 | 1.38 | 1.24 | 9,770 | 46 | 3.2 |
| **97** | 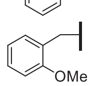 |  | 2.16 | 1.62 | 0.98 | > 100,000 | 35 | 3.6 |
| **98** | 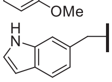 | $CH_3$– | 6.40 | 3.97 | 3.51 | 8,170 | 102 | 11.7 |
| **99** | 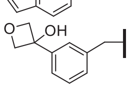 | $CH_3$– | 7.05 | 4.54 | 3.75 | 23,950 | 20 | 28.5 |
| **100** | 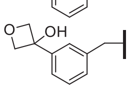 | 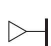 | 3.57 | 3.05 | 1.53 | 5,560 | 22 | 11.75 |
| **101** | 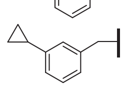 |  | 3.15 | 1.14 | 0.71 | > 100,000 | 54 | 3.25 |
| **102** | 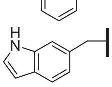 |  | 3.91 | 3.35 | 3.50 | 9,210 | 187 | 12 |
| **103** | 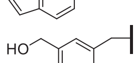 |  | 1.00 | 2.79 | 1.03 | 27,830 | 19 | 11.34 |
| **104** | 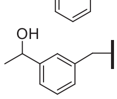 |  | 0.89 | 2.04 | 0.65 | 4,960 | 6.8 | 7.39 |

**Table 8**
Secondary Phase II synthesis and SAR of $R^6$ analogs combined with best $R^4$ and benzyl $R^1$ groups. Activities provided are $EC_{50}$ values (nM) in the indicated pseudotyped virus assays. Cytotoxicity is given as $CC_{50}$ in Vero cells (7 days). HLM data is the observed half-life ($T_{1/2}$ (min)) in a human liver microsome assay. Aqueous solubility (μM) was measured at pH 7.4.

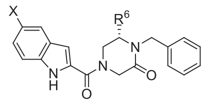

| Compd. | $R^6$ | X | p-LASV | p-MACV | p-JUNV | $CC_{50}$ (nM) | HLM | Solubility |
|---|---|---|---|---|---|---|---|---|
| **105** | 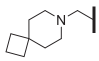 | 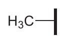 | 11.87 | 17.18 | > 25 | 7,800 | N/A | 12.30 |
| **106** | 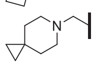 |  | 10.50 | 15.58 | 2.33 | 3,400 | 156 | 7.70 |
| **107** | 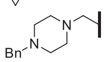 | 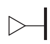 | 15.10 | 5.09 | 5.55 | 5,500 | N/A | 12.86 |
| **108** | 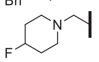 | 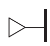 | 4.13 | 11.32 | 3.64 | 24,450 | 23 | 12.35 |

**Table 9**
Collection of prioritized compounds expressing potent, broad spectrum activity (< 10 nM $EC_{50}$ activity against pLASV, pMACV and pJUNV) and HLM metabolic half-life ($T_{1/2}$) > 45 min with indicated aqueous solubility (μM) at pH 7.4 and pJUNV (Candid-1) $EC_{50}$ activity.

| | Compd. | p-LASV | p-MACV | p-JUNV | p-JUNV (Candid-1) | HLM | Solubility |
|---|---|---|---|---|---|---|---|
| 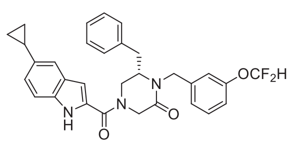 | **66** | 2.12 | 6.81 | 4.05 | N/A | 77 | 6.2 |
| 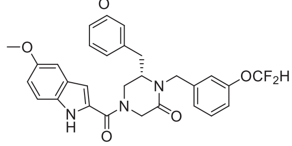 | **46** | 0.94 | 1.85 | 0.75 | 710.3 | 59 | 7.2 |
| 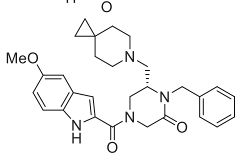 | **79** | 2.99 | 4.53 | 1.25 | 56.2 | 52 | 28.2 |
| 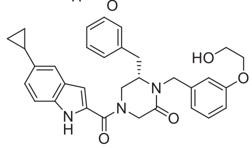 | **95** | 7.72 | 1.08 | 2.16 | 272.9 | 50 | 9.4 |
| 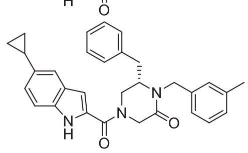 | **96** | 0.94 | 1.38 | 1.24 | 356 | 46 | 3.2 |
| 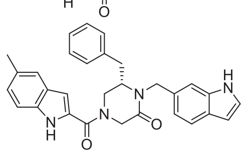 | **98** | 6.40 | 3.97 | 3.51 | 48.4 | 102 | 11.7 |
| 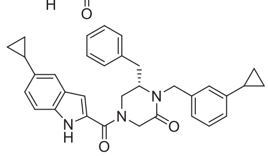 | **101** | 3.15 | 1.14 | 0.71 | 173.2 | 54 | 3.25 |
| 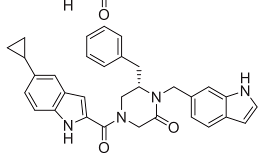 | **102** | 3.91 | 3.35 | 3.5 | 181.5 | 187 | 12 |

## Acknowledgements

We gratefully acknowledge the financial support of the National Institutes of Health (R43AI112097 to K.M and M.B.P.; R44AI112097 to G.H.; CA042056 to D.L.B.; AI074818 and AI065357 to J.H.N) and the generous gifts of arenavirus glycoprotein plasmid constructs and pseudotyped vectors from Juan Carlos de la Torre and Brian Hjelle. The replicative Tacaribe virus TRVL-11573 and monoclonal anti-JUNV, clone MA03-BE06 were obtained from BEI Resources, NIAID, NIH.

## Appendix A. Supplementary data

Supplementary data to this article can be found online at https://doi.org/10.1016/j.bmcl.2019.08.024.

## References

1. Isaacson M. *Clin Infect Dis.* 2001;33:1707.
2. Jahrling PB, Geisbert TW. *Nat Med.* 2004;10:S110.
3. Emonet SF, de la Torre JC, Domingo E, Sevilla N. *Infect Genet Evol.* 2009;9:417.
4. Cajimat MNB, Milazzo ML, Rollin PE, et al. *Virus Res.* 2009;140:24.
5. Pontremoli C, Forni D, Sironi M. *Curr Opin VIrol.* 2018;34:18.
6. Fichet-Calvet E, Rogers DJ. *PLoS Negl Trop Dis.* 2009;3:e388.
7. Borio L, Inglesby T, Peters CJ, et al. *JAMA.* 2002;287:2391.
8. McCormick JB, Fisher-Hoch SP. *Curr Top Microbiol Immunol.* 2002;262:75.
9. Ogbu O, Ajuluchukwu E, Uneke CJ. *J Vector Dis.* 2007;44:1.
10. Khan SH, Goba A, Chu M, et al. *Antiviral Res.* 2008;78:103.
11. Cummins D, McCormick JB, Bennett D, et al. *JAMA.* 1990;264:2093.
12. Macher AM, Wolfe MS. *Emerg Infect Dis.* 2006;12:835.
13. Idemyor VJ. *Natl Med Assoc.* 2010;102:1243.
14. Ibekwe TS, Okokhere PO, Asogun D, et al. *Eur Arch Otorhinolaryngol.* 2011;268:197.
15. McCormick JB, King IJ, Webb PA, et al. *N Engl J Med.* 1986;314:20.
16. Nomura H, Tanimoto H, Kajiwara E, et al. *J Gastroenterol Hepatol.* 2004;19:312.
17. Fuster D, Huertas JA, Gomez G, et al. *Antivir Ther.* 2005;10:841.
18. Bolken TC, Laquerre S, Zhang Y, et al. *Antiviral Res.* 2006;69:86.
19. Larson RA, Dai D, Hosack VT, et al. *J Virol.* 2008;82:10768.
20. Lee AM, Rojek JM, Spiropoulou CF, et al. *J Biol Chem.* 2008;283:18734.
21. Cashman KA, Smith MA, Twenhafel, et al. *Antiviral Res.* 2011;90:70.
22. Thomas CJ, Casquilho-Gray HE, York J, et al. *J Biol Chem.* 2011;286:6192.
23. Nunberg JH, York J. *Viruses.* 2012;4:83.
24. Rojek JM, Spiropoulou CF, Kunz S. *Virology.* 2006;349:476.
25. Pasquato A, Kunz S. *Expert Opin Drug Discov.* 2016;11:383.
26. Whitby LR, Lee AM, Kunz S, Oldstone MB, Boger DL. *Bioorg Med Chem Lett.* 2009;19:3771.
27. Lee AM, Pasquato A, Kunz A. *Virology.* 2011;411:163.
28. Kan T, Fukuyama T. *Chem Commun.* 2004:353.
29. Abdel-Magid AF, Carson KG, Harris BD, Maryanoff CA, Shah RD. *J Org Chem.* 1996;61:3849.
30. Zafrani Y, Yeffet D, Sod-Moriah G, et al. *J Med Chem.* 2017;60:797.
31. Madu IG, Files M, Garaibeh DM, et al. *PLoS Pathog.* 2018;14(12):e1007439.
32. Albarino CG, Bird BH, Chakrabarti AK, et al. *J Virol.* 2011;19:10404.